JOURNAL OF APPLIED PHYSICS 115, 083505 (2014)

Swelling dynamics of a thin elastomeric sheet under uniaxial pre-stretch

A. Lucantonio,[1,a)] P. Nardinocchi,[1] and H. A. Stone[2]
[1]Dipartimento di Ingegneria Strutturale e Geotecnica, Sapienza-Università di Roma, Rome, Italy
[2]Department of Mechanical and Aerospace Engineering, Princeton University, Princeton, New Jersey 08544, USA

(Received 12 December 2013; accepted 11 February 2014; published online 25 February 2014)

It has been demonstrated experimentally that pre-stretch affects the swelling of an elastomeric membrane when it is exposed to a solvent. We study theoretically the one-dimensional swelling of a pre-stretched thin elastomeric sheet, bonded to an impermeable rigid substrate, to quantify the influence of pre-stretch. We show that the solvent uptake increases when pre-stretch increases, both at equilibrium and during the swelling transient, where it exhibits two different scaling regimes. The coupling between the solvent uptake and pre-stretch may be practically exploited to design soft actuators where the swelling-induced deformations can be controlled by varying the pre-stretch. © *2014 AIP Publishing LLC*. [http://dx.doi.org/10.1063/1.4866576]

I. INTRODUCTION

Soft active materials have been employed to realize diverse actuators,[1–3] where deformations and displacements are triggered through a wide range of external stimuli (electric field, pH, temperature, solvent absorption). The functionality of such actuators critically depends on the capability of achieving prescribed changes in shape and size of the system. In particular, in gel-based actuators, the shape and the size of the structures are related to the spatial distribution of solvent inside the gel and to the magnitude of the solvent uptake.

Currently, several approaches to the shape control of swelling materials are being pursued, which often involve materials in the form of thin non-homogeneous sheets.[4–6] Recently, we have proposed an alternative approach[7] for shape manipulation based on a chemically homogeneous elastomeric membrane and on the combination of solvent stimulation with applied pre-stretch. For this approach, it is crucial to quantify how the pre-stretch affects the swelling dynamics and the equilibrium swelling. However, whereas the influence of strain on swelling was investigated from an experimental viewpoint already around 1950,[8,9] limited progress has been made on the theoretical side, especially as regards the effect of the pre-stretch on the dynamics of swelling.

To address these issues, we study a model problem involving the one-dimensional swelling of a thin elastomeric layer that is pre-stretched and bonded to an impermeable rigid substrate. The structure of the problem allows the reduction of the governing equations of the problem to one nonlinear time-dependent partial differential equation (PDE). Almost the same equation governs the uniaxial creep of a confined gel layer,[10] where it was shown that such an equation admits a self-similar solution for the swelling stretch at early times. Here, we identify a new scaling regime for the dynamics of solvent uptake corresponding to intermediate times during the swelling transient. Moreover, we elucidate the dependence of the equilibrium solvent uptake on the pre-stretch by providing an explicit formula that may be practically employed in the design of soft actuators.

II. STRETCHING AND SWELLING PROCESSES

For the model problem, let us consider a stress-free and dry thin elastomeric sheet $\mathcal{B}_d$, with length ℓ_d, width w_d, and thickness $h_d \ll \ell_d, w_d$, which is stretched along its longitudinal axis $\mathbf{e}_1$, while allowed to contract laterally. Subsequently, the sheet is bonded to a rigid and impermeable substrate, adhering to the sheet's bottom surface (Figs. 1(a) and 1(b)). The stretched and dry sheet $\mathcal{B}_\sigma$ has a deformed length $\ell_\sigma = \bar{\lambda}\,\ell_d$, with $1 \le \bar{\lambda} \le 4$ the applied pre-stretch. Due to the incompressibility of the elastomer, the transverse stretch $\bar{\lambda}_\perp$ is such that $\bar{\lambda}_\perp = 1/\sqrt{\bar{\lambda}}$; thus, $\mathcal{B}_\sigma$ has smaller thickness $h_\sigma = \bar{\lambda}_\perp h_d < h_d$ and width $w_\sigma = \bar{\lambda}_\perp w_d < w_d$ than $\mathcal{B}_d$.

The homogeneous deformation gradient $\bar{\mathbf{F}}$ and (reference) stress $\bar{\mathbf{S}}$ that characterize the stretched configuration are

$$\bar{\mathbf{F}} = \bar{\lambda}\mathbf{e}_1 \otimes \mathbf{e}_1 + \bar{\lambda}_\perp\,(\mathbf{I} - \mathbf{e}_1 \otimes \mathbf{e}_1), \quad \bar{\mathbf{S}} = G\bar{\mathbf{F}} - \bar{p}\bar{\mathbf{F}}^{-T}, \quad (1)$$

where G is the shear modulus of the dry elastomer and $\bar{p}$ the constitutively indeterminate pressure field. Here, we have assumed a Neo-Hookean constitutive model for the elastomer. As the balance of forces is trivially satisfied by the homogeneous stress $\bar{\mathbf{S}}$, the solution of the elastic problem is completely determined by the conditions $\bar{\mathbf{S}}\mathbf{e}_\gamma = \mathbf{0}$ on the sheet's boundaries with unit normal $\mathbf{e}_\gamma$ ($\gamma = 2, 3$), which prescribe the pressure field $\bar{p}$ and then allow the determination of the relation between the stretch $\bar{\lambda}$ and the traction $\sigma_1 = \bar{\mathbf{S}}\mathbf{e}_1 \cdot \mathbf{e}_1$

$$\bar{p} = \frac{G}{\bar{\lambda}}, \quad \text{and} \quad \sigma_1 = G\left(\bar{\lambda} - \frac{1}{\bar{\lambda}^2}\right). \quad (2)$$

The stretched sheet $\mathcal{B}_\sigma$ is then exposed all over its free boundary to a solvent with homogeneous chemical potential μ_{ext} (Fig. 1(c)). The sheet undergoes a transient swelling

a)Present address: SISSA-International School for Advanced Studies, via Bonomea 265, 34136 Trieste, Italy. Electronic mail: alessandro.lucantonio@sissa.it.

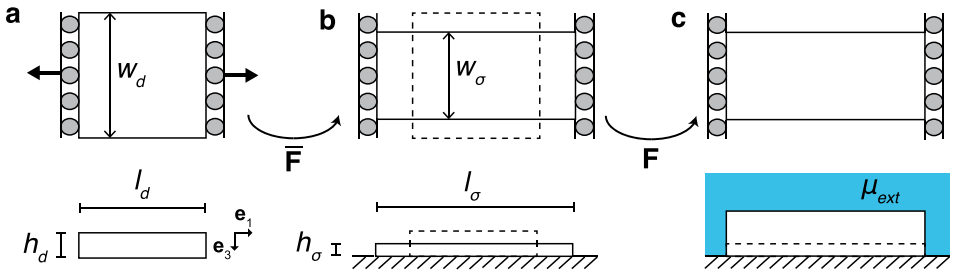

FIG. 1. Sketch of the stretching and swelling processes: (a) The initial dry and stress-free sheet $\mathcal{B}_d$, with its original dimensions. (b) The stretched sheet $\mathcal{B}_\sigma$ on a substrate. (c) A schematic of the swollen sheet in contact with a solvent bath.

process and assumes a sequence of configurations $\mathcal{B}_t$ parameterized by the time $t \in \mathbb{R}$. We describe the swelling dynamics starting from the dry and stretched sheet $\mathcal{B}_\sigma$ within a model devoted to the transient analysis of swelling-induced large deformations in polymer gels.[11] The basic equations of the present theory rest upon the Flory-Rehner representation of the free energy for a swelling polymer,[12] appropriately modified to account for the stress state in the reference configuration $\mathcal{B}_\sigma$.

Because the sheet is thin and confined on its lower surface to a rigid, impermeable substrate, the swelling-induced deformation process is assumed to occur along the thickness direction spanned by the unit vector $\mathbf{e}_3$ and the coordinate $z \in [0, h_\sigma]$. Hence, as usual when similar problems are considered,[10,13] we assume that only the thickness of the sheet undergoes significant variation, so that the swelling-induced deformation gradient $\mathbf{F}$ from the pre-stretched sheet may be represented as

$$\mathbf{F} = (\lambda - 1)\,\mathbf{e}_3 \otimes \mathbf{e}_3 + \mathbf{I}, \tag{3}$$

with $\lambda(z, t)$ the stretch along the thickness due to swelling. Consistent with the reduced representation of $\mathbf{F}$, the incompressibility constraint[11]

$$J := \det \mathbf{F} = 1 + \Omega c \tag{4}$$

takes the form

$$\lambda = 1 + \Omega c, \tag{5}$$

where c is the solvent molar concentration per unit volume in $\mathcal{B}_\sigma$ and Ω the solvent molar volume. For the present problem, the balance equations of forces and solvent reduce to

$$\frac{\partial S_{33}}{\partial z} = 0 \quad \text{and} \quad \frac{\partial c}{\partial t} = -\frac{\partial q}{\partial z}, \tag{6}$$

with $S_{33}(z,t) = \mathbf{S}\mathbf{e}_3 \cdot \mathbf{e}_3$ and $q(z,t) = \mathbf{q} \cdot \mathbf{e}_3$ the only significant components of the stress and the solvent flux, respectively. The constitutive equations for the stress $\mathbf{S}$ and the chemical potential μ can be obtained as the derivatives with respect to $\mathbf{F}$ and c of the following free energy:

$$\Psi(\mathbf{F}, c) = \frac{1}{2} G(\mathbf{F}\bar{\mathbf{F}} \cdot \mathbf{F}\bar{\mathbf{F}} - 3) + \frac{\mathcal{R}T}{\Omega} m(c) - p\,(J - 1 - \Omega c), \tag{7}$$

with

$$m(c) = \Omega c \log \frac{\Omega c}{1 + \Omega c} + \chi \frac{\Omega c}{1 + \Omega c}. \tag{8}$$

Here, we have introduced the universal gas constant $\mathcal{R}$, the environment temperature T, and the dimensionless measure χ of the enthalpy of polymer-solvent mixing. The first two terms of Ψ are the elastic and mixing energies and together define the Flory-Rehner free energy, while the last term enforces the volume constraint (4) through the Lagrange multiplier p, which is the osmotic pressure within the swelling sheet. Specifically, the constitutive equations read[11]

$$\mathbf{S} = \hat{\mathbf{S}}(\mathbf{F}) - pJ\mathbf{F}^{-T} = G\,\mathbf{F}\bar{\mathbf{F}}\,\bar{\mathbf{F}}^T - pJ\mathbf{F}^{-T}, \tag{9}$$

$$\mu = \hat{\mu}(c) + \Omega p = \frac{\mathcal{R}T}{\Omega} m'(c) + \Omega p, \tag{10}$$

$$\mathbf{q} = \hat{\mathbf{q}}(\mathbf{F}, p, c) = -\frac{D\,c}{\mathcal{R}T} (\mathbf{F}^T\mathbf{F})^{-1} \nabla(\hat{\mu}(c) + \Omega p), \tag{11}$$

with

$$m'(c) = \Omega \left(\log \frac{\Omega c}{1 + \Omega c} + \frac{1}{1 + \Omega c} + \frac{\chi}{(1 + \Omega c)^2} \right), \tag{12}$$

and D the diffusion coefficient of the solvent.

Since the top surface ($z = 0$) of the sheet is traction-free, $S_{33}(0, t) = 0$; hence, $S_{33}(z, t) \equiv 0$, and, from Eq. (9), the pressure field takes the form

$$p(z,t) = \frac{G}{\bar{\lambda}}\,\lambda(z,t). \tag{13}$$

The reduced chemical potential $\mu(z, t)$ and solvent flux $q(z, t)$ are prescribed by Eqs. (10) and (11) as

$$\mu = \mathcal{R}T \left(\log\left(1 - \frac{1}{\lambda}\right) + \frac{1}{\lambda} + \frac{\chi}{\lambda^2} \right) + \Omega p, \tag{14}$$

$$q = -\frac{D}{\Omega \mathcal{R}T} \frac{(\lambda - 1)}{\lambda^2} \frac{\partial \mu}{\partial z}, \tag{15}$$

where the incompressibility constraint has been used. Equations $(6)_2$ and (13)–(15) give the evolution for the swelling-induced stretch λ, which is to be solved using the boundary and initial conditions.

Introducing the characteristic time and length $\tau_\sigma = h_\sigma^2/D$ and h_σ, respectively, and the corresponding non-dimensional time $\tau = t/\tau_\sigma$ and thickness coordinate $\zeta = z/h_\sigma$, the evolution equation is

$$\frac{\partial \lambda}{\partial \tau} = \frac{\partial}{\partial \zeta} \left\{ \left[\frac{N\Omega}{\bar{\lambda}} \frac{1}{\lambda} \left(1 - \frac{1}{\lambda}\right) + \frac{1 - 2\chi}{\lambda^4} + \frac{2\chi}{\lambda^5} \right] \frac{\partial \lambda}{\partial \zeta} \right\}, \tag{16}$$

where $N\Omega = G\Omega/\mathcal{R}T$. As the substrate ($\zeta = 1$) is impermeable and the top face of the sheet is assumed to be in equilibrium with the solvent bath, the boundary conditions for Eq. (16) are

$$\mu(0,\tau) = \mu_{ext}, \quad \frac{\partial\lambda}{\partial\zeta}(1,\tau) = 0. \tag{17}$$

Finally, at time $\tau = 0$ the sheet is dry; we assume the following initial condition to overcome the singularity of the Flory-Rehner free energy[12] at the dry state ($\lambda = 1$):

$$\lambda(\zeta,0) \approx 1 \quad \text{for} \quad 0 < \zeta < 1. \tag{18}$$

The initial-boundary value problem (16)–(18) can be solved numerically for different values of $\bar{\lambda}$, once μ_{ext}, $N\Omega$, and χ are specified.

We study the equilibrium solution and the dynamics of Eqs. (16)–(18) as a function of the pre-stretch $\bar{\lambda}$. In particular, with the goal of discussing the dependence of swelling on the pre-stretch, we introduce the relative volume change ϕ with respect to the volume $V_d = \ell_d w_d h_d = \ell_\sigma w_\sigma h_\sigma$ of the dry elastomer

$$\phi(t) = \frac{1}{V_d}\int_{\mathcal{B}_\sigma} \Omega c(z,t)\,\mathrm{d}V = \int_0^1 \Omega c(\zeta,t)\,\mathrm{d}\zeta = \int_0^1 (\lambda(\zeta,t)-1)\,\mathrm{d}\zeta, \tag{19}$$

as a dimensionless measure of solvent uptake.

III. ASYMPTOTIC SOLUTION OF THE SWELLING EQUILIBRIUM

At equilibrium, the chemical potential μ of the solvent within the elastomer is homogeneous and equal to the chemical potential μ_{ext} of the external solvent: $\mu(z,t) = \mu_{ext}$. Without loss of generality, we assume that the external solvent is in equilibrium with its own vapor: $\mu_{ext} = 0$; thus, Eqs. (13) and (14), and the equilibrium condition on the chemical potential give

$$\log\left(1 - \frac{1}{\lambda_\infty}\right) + \frac{1}{\lambda_\infty} + \frac{\chi}{\lambda_\infty^2} + \frac{N\Omega}{\bar{\lambda}}\,\lambda_\infty = 0, \tag{20}$$

where λ_∞ is the swelling-induced stretch attained at equilibrium. In practice, $N\Omega = 10^{-5} - 10^{-2}$ and $\chi = 0.1$–0.5 for good solvents; with $N\Omega$ and χ varying in such ranges, the equilibrium stretch $\lambda_\infty \gg 1$ (that is, $1/\lambda_\infty \ll 1$), and Eq. (20) can be approximated as

$$\frac{N\Omega}{\bar{\lambda}}\,\lambda_\infty^4 + \left(\chi - \frac{1}{2}\right)\lambda_\infty - \frac{1}{3} + O(\lambda_\infty^{-1}) = 0. \tag{21}$$

Equation (21) defines a singular perturbation problem in the small parameter $\varepsilon = N\Omega$. Seeking a perturbation expansion solution of Eq. (21) in the form $\lambda_\infty = \varepsilon^{-1/3}\Lambda_0 + \Lambda_1 + O(\varepsilon^{1/3})$, we obtain

$$\lambda_\infty \sim \left(\frac{1-2\chi}{2N\Omega}\right)^{1/3}\bar{\lambda}^{1/3} + \frac{2}{9}\,\frac{1}{(1-2\chi)}. \tag{22}$$

Equation (22) shows that, at leading order, the swelling equilibrium solution depends on the pre-stretch $\bar{\lambda}$, through the parameter $\alpha = (1-2\chi)/2N\Omega$. The parameter α has already been introduced[12,14] and represents the leading order of the swelling equilibrium solution, in the absence of pre-stretch. Formula (22) agrees very well with the numerical solution of the exact equilibrium equation (20), as shown in Fig. 2. We note that the equilibrium stretch λ_∞ increases when the pre-stretch $\bar{\lambda}$ increases: this trend can be explained by noting that the osmotic pressure p, which contrasts the solvent uptake, decreases with the pre-stretch (Eq. (13)), thus favoring the swelling of the elastomer. Indeed, the decrease in the osmotic pressure lowers the chemical potential μ inside the elastomer (Eq. (14)) and thus increases the magnitude of the driving force for the solvent uptake, that is the difference between μ and the external chemical potential μ_{ext}. Moreover, the equilibrium stretch increases, as can be expected, when the elastomer becomes softer ($N\Omega$ decreases), or when the affinity between the solvent and the polymer increases (χ decreases).

IV. SCALING ANALYSIS OF THE SWELLING DYNAMICS AND THE SOLVENT UPTAKE

We now consider Eq. (16) for the stretch $\lambda(\zeta, \tau)$. For early times, $\tau \ll 1$, swelling involves only the regions of the thickness near the top surface (which is in contact with the solvent) and the finite thickness of the layer does not affect solvent diffusion. Hence, because the problem has no intrinsic length scale, the stretch λ evolves according to a self-similar profile: $\lambda(\zeta, \tau) = \psi(\xi)$, with $\xi = \zeta/\sqrt{\tau}$, $0 \le \xi \le \infty$. Previously, it was shown[10] that Eq. (16) for $\bar{\lambda} = 1$, i.e., in the absence of pre-stretch, admits a self-similar solution. A nonlinear ordinary differential equation (ODE) is obtained by substituting the self-similar representation into Eq. (16) and is solved numerically. Then, the solvent uptake for early times may be evaluated using Eq. (19) as

$$\phi(\tau) = \sqrt{\tau}\int_0^\infty (\psi(\xi) - 1)\,\mathrm{d}\xi. \tag{23}$$

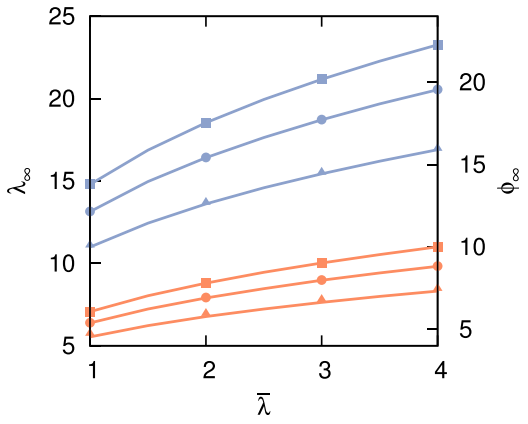

FIG. 2. Equilibrium stretch λ_∞ and equilibrium solvent uptake $\phi_\infty = \lambda_\infty - 1$ versus pre-stretch $\bar{\lambda}$ as computed from the numerical solution of Eq. (20) (solid lines) or from the asymptotic solution Eq. (22) (symbols), for $N\Omega = 10^{-4}$ (blue) and $N\Omega = 10^{-3}$ (orange), and for different values of χ: 0.2 (squares), 0.3 (circles), and 0.4 (triangles).

We verified numerically that the integral in Eq. (23) varies between 0.613 and 0.62 for $1 \leq \bar{\lambda} \leq 4$ and thus is almost independent of the pre-stretch; hence, the solvent uptake as a function of τ is independent of the pre-stretch and follows the scaling law $\phi \propto \tau^{1/2}$ for early times.

To analyze the swelling dynamics for intermediate times, $\tau = O(1)$, beyond the early transient, we use for the stretch the same scaling introduced for the equilibrium solution: $\lambda = \varepsilon^{-1/3} y$; then, the governing PDE equation (16) is

$$\frac{\partial y}{\partial \tau} = \frac{\partial}{\partial \zeta}\left\{\left[\frac{\varepsilon^{4/3}}{y}\left(\frac{1-2\chi}{y^3}+\frac{1}{\bar{\lambda}}\right)+\frac{\varepsilon^{5/3}}{y^2}\left(\frac{2\chi}{y^3}-\frac{1}{\bar{\lambda}}\right)\right]\frac{\partial y}{\partial \zeta}\right\}, \tag{24}$$

which, up to terms $O(\varepsilon^{4/3})$ and in terms of λ, becomes

$$\frac{\partial \lambda}{\partial \tau} = \frac{\partial}{\partial \zeta}\left[\frac{1}{\lambda}\left(\frac{\varepsilon}{\bar{\lambda}}+\frac{1-2\chi}{\lambda^3}\right)\frac{\partial \lambda}{\partial \zeta}\right]. \tag{25}$$

Equation (25) represents the evolution equation for the stretch in the intermediate time regime, where swelling is not limited to the top regions of the thickness, as it was in the early transient, and the thickness h_σ of the stretched elastomer sets the length scale for the dynamics.

We can eliminate the parameters in Eq. (25) by scaling the stretch λ with the leading term $\Lambda = \alpha^{1/3}\bar{\lambda}^{1/3}$ of the swelling equilibrium solution (22) and by introducing a new characteristic time $\tau_0 = \Lambda\,\bar{\lambda}/\varepsilon$

$$\frac{\partial \hat{\lambda}}{\partial \hat{\tau}} = \frac{\partial}{\partial \zeta}\left[\frac{1}{\hat{\lambda}}\left(1+\frac{2}{\hat{\lambda}^3}\right)\frac{\partial \hat{\lambda}}{\partial \zeta}\right], \tag{26}$$

with $\hat{\lambda} = \lambda/\Lambda$ and $\hat{\tau} = \tau/\tau_0$. The corresponding boundary conditions are $\hat{\lambda} \approx 1$ at $\zeta = 0$ and $\partial\hat{\lambda}/\partial\zeta = 0$ at $\zeta = 1$. The initial condition for $\hat{\lambda}$ should match the self-similar profile for the early transient; however, since we are interested in discussing the scaling features of the solution of Eq. (26) for intermediate times, without solving the equation, only boundary conditions of Eq. (26) are relevant.

Equation (26) and the corresponding boundary conditions are independent of $\bar{\lambda}$; hence, we also expect the rescaled solution $\hat{\lambda}(\zeta, \hat{\tau})$ computed from the solution λ of problems (16)–(18) to be independent of the pre-stretch $\bar{\lambda}$, in the intermediate time regime. Indeed, we evaluated $\hat{\lambda}(\zeta, \hat{\tau})$, for fixed $N\Omega = 10^{-3}$ and $\chi = 0.2$, at $\zeta = 1/2$, $\zeta = 1/10$, and $\zeta = 1/100$ for different values of $\bar{\lambda}$ varying from 1 to 4, and showed that the solution curves collapse on three master curves (Fig. 3(a)). We verified that an analogous collapse[15] occurs for different values of $N\Omega$ and χ. Moreover, these master curves, as well as the curves corresponding to other spatial positions not shown in Fig. 3(a), have the same slope in the $\log\hat{\lambda} - \log\hat{\tau}$ plane, except for a small region close to the boundary $\zeta = 0$. Hence, the scaled stretch evolves in time following the scaling law $\hat{\lambda} \propto \hat{\tau}^{\beta}$, almost independently of the space coordinate ζ, as confirmed by the plot of $\hat{\lambda}/\hat{\tau}^{\beta}$ for several intermediate times $\hat{\tau} \in \mathcal{I} = [10^{-3}, 10^{-2}]$ depicted in Fig. 3(b). We found numerically that $\beta \approx 0.24$.

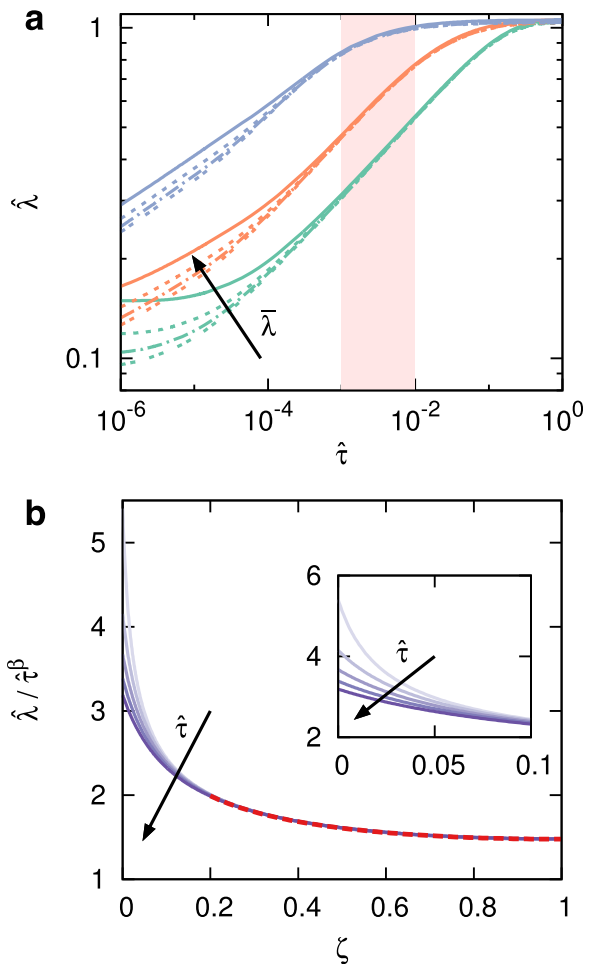

FIG. 3. Scaling behavior of the stretch $\hat{\lambda} = \lambda/\Lambda$ for intermediate times, with $\chi = 0.2$, $N\Omega = 10^{-3}$. The results are obtained from the numerical solution of the problem (16)–(18). (a) The solid, dashed, and dotted lines, representing, respectively, the stretch $\hat{\lambda}$ evaluated at $\zeta = 1/2$ (green), $\zeta = 1/10$ (orange), and $\zeta = 1/100$ (blue), for different values of the pre-stretch $\bar{\lambda} = 1, 2, 3, 4$, collapse on three master curves, in the intermediate time regime. (b) Quasi self-similar profile of $\hat{\lambda}$ for intermediate times. The solid lines correspond to $\hat{\lambda}/\hat{\tau}^{\beta}$, $\beta = 0.24$ at different times in the interval $10^{-3} \leq \hat{\tau} \leq 10^{-2}$ (shaded area in (a)). The dashed line is the analytical solution (29) of the ODE (28) where the time-dependent terms are neglected, for $\beta = 1/4$ and $0.2 \leq \zeta \leq 1$.

According to the observed scaling behavior of $\hat{\lambda}$, we assume that the following representation holds, for $\hat{\tau} \in \mathcal{I}$:

$$\hat{\lambda}(\zeta, \hat{\tau}) = \begin{cases} \hat{\tau}^{\beta} g(\zeta, \hat{\tau}), & 0 \leq \zeta \leq \delta, \\ \hat{\tau}^{\beta} f(\zeta), & \delta \leq \zeta \leq 1, \end{cases} \tag{27}$$

where δ is the characteristic length of the region where $\hat{\lambda}/\hat{\tau}^{\beta}$ shows a significant dependence on $\hat{\tau}$ (in Fig. 3(b), $0.1 \leq \delta \leq 0.2$). To estimate analytically the value of the scaling exponent β, we substitute expression (27) valid for $\delta \leq \zeta \leq 1$ in the governing equation for intermediate times (26)

$$\left(\frac{2}{f^4}+\frac{\hat{\tau}^{3\beta}}{f}\right)f'' - \left(\frac{8}{f^5}+\frac{\hat{\tau}^{3\beta}}{f^2}\right)(f')^2 - \beta\,\hat{\tau}^{4\beta-1} f = 0. \tag{28}$$

The last term becomes independent of $\hat{\tau}$ with the choice $\beta = 1/4$, while the remaining time-dependent terms are

proportional to $\hat{\tau}^{3/4} \ll 1$, for $\hat{\tau} \in \mathcal{I}$. We expect the solution to depart from the scaling regime when $\hat{\tau} = O(1)$. Note that the value of β estimated analytically is very close to the value of the scaling exponent found numerically.

Equation (28) can be solved analytically for $\beta = 1/4$ and neglecting the time-dependent terms

$$\frac{\sqrt{F^2-1} - F^2 \arctan\left(\frac{1}{\sqrt{F^2-1}}\right)}{2F^2} = \frac{(f^\star)^2}{\sqrt{8}}(1-\zeta) - \frac{\pi}{4}, \quad (29)$$

where $F = f/f^\star, f^\star = f(1)$ and the boundary condition $f'(1) = 0$ has been imposed. Equation (29) is plotted in Fig. 3(b), where $f^\star$ has been chosen equal to the value of $\hat{\lambda}/\hat{\tau}^\beta$ at $\zeta = 1$ computed from the numerical solution of problems (16)–(18). The agreement between $f(\zeta)$ given by Eq. (29) and $\hat{\lambda}/\hat{\tau}^\beta$ obtained from the numerical solution of the full problem further supports the existence of a scaling regime for intermediate times.

The scaling behavior of the stretch for intermediate times induces an analogous behavior for the solvent uptake. Indeed, using the representation (27), the solvent uptake at intermediate times may be computed as

$$\phi(\hat{\tau}) = \Lambda\, \hat{\tau}^\beta \left(\int_0^\delta g(\zeta, \hat{\tau})\, \mathrm{d}\zeta + \int_\delta^1 f(\zeta)\, \mathrm{d}\zeta \right) - 1. \quad (30)$$

We assume that the dependence of g on $\hat{\tau}$ is weak, so that the function may be approximated with the zeroth-order term of its Taylor expansion in $\hat{\tau}$ about a time $\hat{\tau}_0 \in \mathcal{I}$

$$\begin{aligned} \phi &\sim \Lambda\, \hat{\tau}^\beta \left(\int_0^\delta g(\zeta, \hat{\tau}_0)\, \mathrm{d}\zeta + \int_\delta^1 f(\zeta)\, \mathrm{d}\zeta \right) - 1 \\ &= \Lambda \left(\frac{\tau}{\tau_0} \right)^\beta \mathcal{F}(\hat{\tau}_0) - 1\,, \end{aligned} \quad (31)$$

where $\mathcal{F}(\hat{\tau}_0)$ is estimated from the numerical solution of problems (16)–(18) as

$$\mathcal{F}(\hat{\tau}_0) = \frac{1}{\hat{\tau}_0^\beta} \int_0^1 \hat{\lambda}(\zeta, \hat{\tau}_0)\, \mathrm{d}\zeta. \quad (32)$$

The value of the integral is numerically evaluated to be between 1.8 and 1.9 for $\hat{\tau}_0 \in \mathcal{I}$ and is thus almost independent of $\hat{\tau}_0$. Furthermore, the quantity Λ/τ_0^β varies in the range of 0.809–0.823, when $\chi = 0.2$ and $N\Omega = 10^{-3}$ and $1 \le \bar{\lambda} \le 4$, and thus it is weakly affected by the pre-stretch, as may be verified numerically.[15] Hence, the dimensionless solvent uptake given by Eq. (31) is independent of the pre-stretch, when ϕ is represented as a function of τ (Fig. 4(a)). We have already noted that the same holds for ϕ as a function of τ for early times (Eq. (23)). The solvent uptake curves for different values of $\bar{\lambda}$ computed from the numerical solution of the full problem (16)–(18) collapse on the curves corresponding to the scaling laws (23) and (31), thus confirming the independence of ϕ on $\bar{\lambda}$, for early and intermediate times, when ϕ is plotted against the time variable τ.

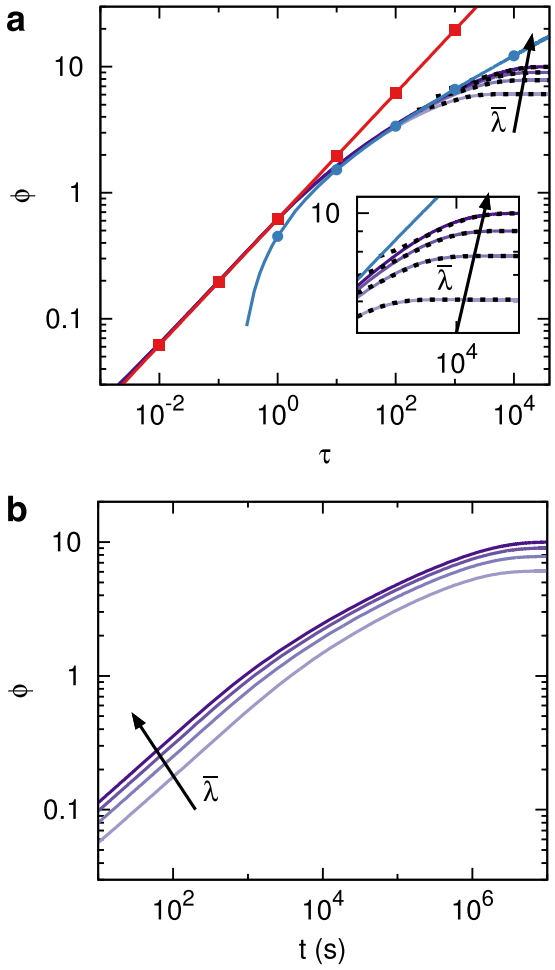

FIG. 4. Scaling behavior of the solvent uptake ϕ as a function of (a) τ and of (b) the physical time t, with $\chi = 0.2$, $N\Omega = 10^{-3}$. The scaling law corresponds to Eq. (23) for the early transient (squares) and to Eq. (31) for intermediate times (circles). The lines without symbols in (a) and (b) represent the solvent uptake computed from the numerical solutions of the problems (16)–(18) for $\bar{\lambda} = 1, 2, 3, 4$. The dashed lines represent the solvent uptake for late times given in Eq. (37), where the constant C is adjusted to fit the numerical solution. For the definition of the time scale $\tau_\sigma = h_d^2/(\bar{\lambda} D)$, the following values for the parameters are chosen: $D = 8 \times 10^{-10}\,\mathrm{m}^2/\mathrm{s}$ and $h_d = 1\,\mathrm{mm}$.

To explicitly quantify the effect of the pre-stretch on the dynamics of swelling, it is necessary to express ϕ in terms of the dimensional time t, because the time scale $\tau_\sigma = h_d^2/(\bar{\lambda} D)$ used to nondimensionalize the time depends on the pre-stretch

$$\phi(t) \sim \frac{\Lambda}{\tau_0^\beta} \left(\frac{t}{\tau_\sigma} \right)^\beta \mathcal{F}(\hat{\tau}_0) - 1. \quad (33)$$

The solvent uptake in Eq. (33) depends on the pre-stretch only through the time scale τ_σ (as we have seen that Λ/τ_0^β and $\mathcal{F}(\hat{\tau}_0)$ are almost independent of $\bar{\lambda}$) and this dependence is evident when we represent ϕ computed from the full problem as a function of t (Fig. 4(b)). We conclude that the solvent uptake increases when the pre-stretch increases, at early and intermediate times during the swelling transient, because of a geometrical effect, i.e., the reduction in the thickness $h_\sigma = h_d/\sqrt{\bar{\lambda}}$, which makes the time scale $\tau_\sigma = h_\sigma^2/D$ decrease with $\bar{\lambda}$.

For late times, $\tau = O(\tau_0)$, $\tau_0 \gg 1$, the solvent uptake deviates from the scaling law (31) as the system approaches to equilibrium. Indeed, when $\hat{\tau} = O(1)$ the time-dependent terms in Eq. (28) become comparable with the other terms, so the scaling hypothesis (27) is no longer appropriate. Because τ_0 increases with $\bar{\lambda}$, the late time regime sets in later as the pre-stretch increases (Fig. 4(a)). Note that the intermediate regime is distinguished from the approach to equilibrium, because the time scales that correspond to such regimes are separate.

In the late time regime, the effective diffusivity, i.e., the term that multiplies $\partial\lambda/\partial\zeta$ in Eq. (16), tends to the (approximate) equilibrium value

$$\tilde{D} = \frac{N\Omega}{\bar{\lambda}}\frac{1}{\Lambda}\left(1 - \frac{1}{\Lambda}\right) + \frac{1-2\chi}{\Lambda^4} + \frac{2\chi}{\Lambda^5}. \tag{34}$$

By linearizing Eq. (16) about the leading-order equilibrium stretch Λ, we obtain a diffusion equation that governs the approach to equilibrium for the incremental stretch $\tilde{\lambda} = \lambda - \Lambda$

$$\frac{\partial\tilde{\lambda}}{\partial\tau} = \tilde{D}\frac{\partial^2\tilde{\lambda}}{\partial\zeta^2}, \quad \tilde{\lambda} \ll 1, \tag{35}$$

subject to the boundary conditions $\tilde{\lambda} \approx 0$ at $\zeta = 0$ and $\partial\tilde{\lambda}/\partial\zeta = 0$ at $\zeta = 1$. The solution of this problem by separation of variables is

$$\begin{aligned} \tilde{\lambda}(\zeta,\tau) &= \sum_{n=0}^{\infty} A_n \exp\left[-\frac{\pi^2}{4}(2n+1)^2\tilde{D}\,\tau\right]\mathcal{Z}_n(\zeta), \\ \mathcal{Z}_n(\zeta) &= \sin\left[\frac{\pi}{2}(2n+1)\zeta\right]. \end{aligned} \tag{36}$$

Hence, considering only the slowest decaying mode $n = 0$ of this expansion, the solvent uptake for late times is

$$\phi(t) \approx \Lambda - 1 + C\exp\left(-\frac{\pi^2}{4}\tilde{D}\,\frac{t}{\tau_\sigma}\right). \tag{37}$$

The amplitude C of the first mode should be computed from an initial condition, but here we adjust its value to fit the numerical solution of the problem (16)–(18). Equation (37) is plotted in Fig. 4(a), for different values of $\bar{\lambda}$, and agrees well with the numerical solution. A straightforward analysis shows that $\tilde{D}/\tau_\sigma$ decreases with $\bar{\lambda}$, thus the approach to equilibrium is slower when pre-stretch increases.

V. CONCLUSIONS

In summary, we have derived an asymptotic solution for the equilibrium swelling of a stretched elastomeric sheet, which has allowed us to discuss the dependence of the equilibrium solvent uptake on the pre-stretch and on the thermodynamic and elastic parameters of the system. Furthermore, we have studied the complete dynamics of swelling, from early times to the approach to equilibrium, and identified two scaling regimes for the dynamics of solvent uptake, corresponding to early and intermediate times.

The semi-analytical study performed here confirms qualitatively previous results[7–9] reporting that the solvent uptake increases when pre-stretch increases, both during the swelling transient and at equilibrium. Potential applications of the problem presented here include one-dimensional soft actuators, for which the stroke can be tuned by varying the pre-stretch of the elastomer.

ACKNOWLEDGMENTS

A.L. and P.N. thank MIUR for support (PRIN 2009 Project No. 200959L72B). H.A.S. thanks the NSF for support via grant CBET-1132835 and Sapienza-Università di Roma for the opportunity to visit.

[1]M. E. Harmon, M. Tang, and C. W. Frank, Polymer **44**, 4547 (2003).
[2]L. Dong, A. K. Agarwal, D. J. Beebe, and H. Jiang, Nature **442**, 551 (2006).
[3]*Biomedical Applications of Electroactive Polymer Actuators*, edited by F. Carpi and E. Smela (Wiley, 2009).
[4]M. A. Dias, J. A. Hanna, and C. D. Santangelo, Phys. Rev. E **84**, 036603 (2011).
[5]J. Kim, J. A. Hanna, M. Byun, C. D. Santangelo, and R. C. Hayward, Science **335**, 1201 (2012).
[6]Z. L. Wu, M. Moshe, J. Greener, H. Therien-Aubin, Z. Nie, E. Sharon, and E. Kumacheva, Nat. Commun. **4**, 1586 (2013).
[7]A. Lucantonio, M. Roché, P. Nardinocchi, and H. A. Stone, "Buckling dynamics of a solvent-stimulated stretched elastomeric sheet," Soft Matter DOI:10.1039/C3SM52941J (published online).
[8]G. Gee, Trans. Faraday Soc. **42**, 585 (1946).
[9]L. R. G. Treloar, Trans. Faraday Soc. **46**, 783 (1950).
[10]W. Hong, X. Zhao, J. Zhou, and Z. Suo, J. Mech. Phys. Solids **56**, 1779 (2008).
[11]A. Lucantonio, P. Nardinocchi, and L. Teresi, J. Mech. Phys. Solids **61**, 205 (2013).
[12]M. Doi, J. Phys. Soc. Jpn. **78**, 052001 (2009).
[13]M. K. Kang and R. Huang, J. Mech. Phys. Solids **58**, 1582 (2010).
[14]H.-H. Dai and Z. Song, Soft Matter **7**, 8473 (2011).
[15]See supplementary material at http://dx.doi.org/10.1063/1.4866576 for the analysis of the scaling regimes for different values of χ and $N\Omega$.